History matching under training-image based geological model constraints

JEF CAERS

Stanford University,
Department of Petroleum Engineering
Stanford, CA 94305-2220

January 2, 2002

Corresponding author
Jef Caers
Stanford University
Petroleum Engineering
Stanford, CA 94305-2220
tel: 1 650 723 1774
e-mail: jef@pangea.stanford.edu

Abstract

History matching forms an integral part of the reservoir modeling work-flow process. Despite the existence of many history matching tools, the integration of production data with seismic and geological continuity data remains a challenge. Geostatistical tools exists for integrating large scale seismic and fine scale well/core data. A general framework for integrating production data with diverse types of geological/structural data is largely lacking. In this paper we develop a new method for history matching that can account for production data constraint by prior geological data, such as the presence of channels, fractures or shale lenses. With multiple-point (mp) geostatistics prior information about geological patterns is carried by training images from which geological structures are borrowed then anchored to the subsurface data. A simple Markov chain iteratively modifies the mp geostatistical realizations until history match. The method is simple and general in the sense that the procedure can be applied to any type of geological environment without requiring a modification of the algorithm.

Introduction

Production data brings an important, yet indirect constraint to the spatial distribution of reservoir variables. Pressure data provides information on the average pore volume and permeability connectivity near wells, while fractional flow data informs the extent of permeability connectivity between wells. Production data rarely suffice however to characterize heterogeneous reservoirs, a large amount of uncertainty still remains after history matching of geostatistical models [1].

History matching is an ill-posed inverse problem attempting to invert reservoir properties from measured flow and pressure data. Solutions to such inverse problems are never unique which allows imparting other sources of data such as provided by seismic surveys and geological interpretation. The non-uniqueness of the history matching problem is well-known and various techniques have been developed that allow integrating production data with geological continuity information in fine scale geostatistical models[2,3,4,5,6,7]. Most of these prior geological models reproduce only the covariance as a measure of geological continuity. Covariance models are rarely sufficient to depict patterns of gfeological continuity consisting of strongly connected, curvi-linear geological objects such as channels or fractures, see for example [8] and [9]. Ideally one would like to possess a single history matching algorithm that can handle diverse type of geological structures.

We propose a pixel-based history matching method that can account for any complex style of geological continuity, not necessarily limited to the two-point statistics of a variogram model. That geological heterogeneity is characterized by multiple-point (mp) patterns and corresponding statistics. The mp patterns are inferred from a training image. A fast sequential simulation algorithm, termed snesim (single normal equation simulation), then borrows those patterns from the training image and anchors them to local subsurface data. Next, the concept of multiple-point geostatistics is combined with a simple one-parameter Markov chain process to address the history matching problem. The transition matrix of this Markov chain is parameterized by a single parameter and modifies gradually and iteratively an initial geology consistent geostatistical realization to match better the production data. The Markov chain is implemented such that the final model honors the imposed training-image

based geological structure. We first review some important concepts in mp geostatistics that allows defining a large variety of prior geological models, then develop the proposed history matching methodology.

Multiple-point geostatistics

Borrowing structures from training images

The snesim algorithm

Traditional to geostatistics, geological continuity is captured through a variogram. A variogram measures the degree of correlation/connectivity or conversely variability between any two locations in space. Since the variogram is only a two-point statistics, it cannot model curvi-linear structures such as channels, nor can it model strong contiguous patterns of connectivities such as fractures. The representation of such complex geological features requires multiple-point statistics, involving jointly more than two locations. The idea behind multiple-point geostatistics is to infer spatial patterns using many spatial locations of a given geometric template scanning a training image or reservoir analog[8,9].

The corresponding algorithm, termed *snesim,* is proposed in [9,10]. It is essentially not different from existing more traditional conditional simulation techniques [11,12], in that it sequentially generates the numerical model, one grid cell after another. The difference comes from the probability distributions from which these pixel values are drawn: in snesim these probabilities are actual proportions inferred from the training image and made conditional to an mp data event. In traditional sequential simulation these probabilities are derived by kriging using a variogram model.

Sequential simulation then allows to generate a number of equiprobable realizations which reproduce the training image pattern of continuity and honor local well-log and seismic data. The snesim approach essentially replaces the variogram modeling by the construction of a training image. A training image would typically be constructed using an unconstrained 3D Boolean simulation, see Fig. 1.

At each node of the simulation grid, denote by $P(A|B)$ the probability model from which the value at that grid cell is drawn, where A could be the event "channel present" at a given grid cell location and B is the set of sample data and previously simulated grid cells used to constrain A. In the sequantial Gaussian simulation (sGs), $P(A|B)$ is a Gaussian distribution with mean and variance determined by a set of (variogram-based) kriging equations. The snesim algorithm follows the same principle of sequential simulation, but the probability model $P(A|B)$ is read from the training image rather than built by kriging from the variogram model. The snesim algorithm then allows generating the patterns found on the training image (see [9] for details).

The various proportions $P(A|B)$ are retrieved from the training image and stored in a dynamic search tree prior to starting the random path [9]. An example of the snesim methodology, using the training image of Fig. 1 is presented in Fig. 2. Note that the training image model need not have the same size as the actual zone being simulated.

Constraining to soft data

The snesim algorithm allows for the integration of secondary information, used by the proposed history matching methodology. For example, seismic inversion procedures allow quantifying from amplitude data the probability of presence of specific facies, see for example [13]. This probabilistic inversion result must then be integrated with finer scale well data and geological prior models as depicted by the training image. Using a notation similar to that above we denote the probability model derived from secondary data as $P(A|C)$, where A is the unknown property at each grid node and C is the secondary data event observed in the neighborhood of that node.

In order to integrate that secondary information C into the snesim algorithm we need to draw from the conditional distribution $P(A|B,C)$ instead of $P(A|B)$, i.e. each simulated value should also depend on the secondary data. To combine $P(A|B)$ and $P(A|C)$ into $P(A|B,C)$, we use the following expression based on an improved form of conditional independence[14]

$$\frac{x}{b} = \frac{c}{a} \tag{1}$$

where

$$x = \frac{1 - P(A|B,C)}{P(A|B,C)}$$

and

$$b = \frac{1 - P(A|B)}{P(A|B)}, c = \frac{1 - P(A|C)}{P(A|C)}, a = \frac{1 - P(A)}{P(A)},$$

$P(A)$ is the global proportion of A occurring, hence a can be interpreted as a prior distance to the event A occurring, prior to knowing the information carried by the event B or C. Indeed if $P(A) = 1$ then the distance $a = 0$ and A is certain to occur. Likewise, the values b and c state the uncertainty about occurrence of A, given information B and C respectively. x is the uncertainty when knowing both B and C. The combined probability $P(A|B,C)$ is derived as follows

$$P(A|B,C) = \frac{1}{1+x} = \frac{a}{a+bc}$$

Based on this expression, an algorithm termed cosnesim has been developed (see [9,13]) which allows generating models constrained to both the geological structure depicted by the training image (information B) and the secondary data C.

Solving the inverse problem

Methodology

We will consider only the case of a binary spatial variable described by an indicator random function model

$$I(\mathbf{u}) = \begin{cases} 1 & \text{if a given facies occurs at } \mathbf{u} \\ 0 & \text{else} \end{cases}$$

where $\mathbf{u} = (x, y, z) \in$ Reservoir, is the spatial location of a grid cell. In a reservoir context $i(\mathbf{u}) = 1$ could mean that channel occurs at location $\mathbf{u}$, while $i(\mathbf{u}) = 0$ indicates non-channel occurrence. In the mp geostatistics context, we denote by A the event $I(\mathbf{u}) = 1$ ("the event occurs") and use D for the production data.

Next, define a non-stationary Markov chain on the entire set of random variables $I(\mathbf{u}), \forall \mathbf{u}$, starting from an initial model $i^{(o)}(\mathbf{u})$, generating iterations $i^{(l)}(\mathbf{u})$ till convergence. Convergence is defined as matching the data D up to a given precision ϵ. To define such Markov

chain, consider the single random variable $I(\mathbf{u})$ at a specific location $\mathbf{u}$. Since $I(\mathbf{u})$ is binary, define the four transition probabilities of a 2×2 non-stationary transition matrix, moving the chain from state (l) to state $(l+1)$ at location $\mathbf{u}$. The chain is parameterized by a single parameter r_D, where $r_D \in [0,1]$ and depends on the data D as follows

$$\Pr\{I^{(l+1)}(\mathbf{u}) = 1 | D, i^{(l)}(\mathbf{u}) = 0\} = r_D \Pr\{I(\mathbf{u}) = 1\}) \tag{2}$$

$$\Pr\{I^{(l+1)}(\mathbf{u}) = 0 | D, i^{(l)}(\mathbf{u}) = 1\} = r_D \Pr\{I(\mathbf{u}) = 0\}) \tag{3}$$

$$\Pr\{I^{(l+1)}(\mathbf{u}) = 1 | D, i^{(l)}(\mathbf{u}) = 1\} = 1 - r_D \Pr\{I(\mathbf{u}) = 0\}$$

and for closure

$$\Pr\{I^{(l+1)}(\mathbf{u}) = 0 | D, i^{(l)}(\mathbf{u}) = 0\} = 1 - r_D \Pr\{I(\mathbf{u}) = 1\}$$

The first two transition probabilities (2) and (3) are the probabilities of changing states (facies) from step (l) to step $(l+1)$; r_D is the relative probability of such change of state, relative to the prior $P(A)$. r_D is a taken as a function of the conditioning data D. The degree of freedom r_D allows moving the model to matching closer the data D. At each iteration, a one-dimensional optimization is carried out to find the value r_D^{opt} that matches best the data D. For any given $r_D \in [0,1]$ at any given current iteration (l) and for all grid cells $\mathbf{u}$ the conditional probability $P(A|D)$ is obtained using the above transition matrix as

$$P(A|D) = r_D P(A) \quad \text{if } i^{(l)}(\mathbf{u}) = 0 \tag{4}$$

$$1 - P(A|D) = r_D(1 - P(A)) \quad \text{if } i^{(l)}(\mathbf{u}) = 1 \tag{5}$$

r_D is the same for all grid cells $\mathbf{u}$. The resulting probability $P(A|D)$ is then combined with thee training image-derived probability $P(A|B)$ using Eq. (1) where $P(A|C)$ is replaced by $P(A|D)$. Note that the resulting realization $i_{r_D}^{(l+1)}(\mathbf{u})$, honors the prior geological continuity as depicted by the training image. Using a simulator of choice, the production data is forward evaluated on $i_{r_D}^{(l+1)}(\mathbf{u})$ and an optimal r_D^{opt} can be selected using any simple one-dimensional optimization method (e.g. the Dekker-Brent method, see [17]). This Markov chain is termed "non-stationary" since r_D changes at each iteration (l).

Two limit cases exist for r_D:

- $r_D = 0$: then the probability for a change is according to Eq. (2)

$$P\{I^{(l+1)}(\mathbf{u}) = 1 - i | D, i^{(l)}(\mathbf{u}) = i\} = 0, \quad \forall i = 0, 1$$

that is $I^{(l+1)}(\mathbf{u}) = I^{(l)}(\mathbf{u})$. Iteration $(l+1)$ does not provide a better match to the data D, hence, one can either stop the iteration or change the random seed s. The latter amounts to starting the chain/iteration over with $i^{(l)}(\mathbf{u})$ as the initial guess.

- $r_D = 1$: then

$$P\{I^{(l+1)}(\mathbf{u}) = 1 | D, i^{(l)}(\mathbf{u}) = 0\} = P(A) = P\{I^{(l+1)}(\mathbf{u}) = 1\}$$

$$P\{I^{(l+1)}(\mathbf{u}) = 0 | D, i^{(l)}(\mathbf{u}) = 1\} = 1 - P(A) = P\{I^{(l+1)}(\mathbf{u}) = 0\}$$

hence the state is changed according to the prior probability of the new state. The combined probability then becomes

$$P(A|B, D) = P(A|B)$$

Consequently the cosnesim algorithm will generate a new realization $i^{(l+1)}(\mathbf{u})$, drawn independently of $i^{(l)}(\mathbf{u})$

Fig. 3 shows an example of five models $i^{(1)}_{r_D}(\mathbf{u})$ generated with different values r_D, starting from the initial model $i^{(o)}(\mathbf{u})$ shown in the top left corner. Note that the bottom right model $i^{(1)}_{r_D=1}(\mathbf{u})$ appears completely independent of $i^{(o)}(\mathbf{u})$.

Another interpretation of r_D

Eqs. (4) and (5) can be recombined into a single equation providing another interpretation of r_D

$$P(A|D) = (1 - r_D) i(\mathbf{u}) + r_D P(A) \quad \in [0, 1] \tag{6}$$

The probability $P(A|D)$ appears as a mixeture of the current realization $i(\mathbf{u})$ and the net-to-gross prior proportion $P(A)$, that mixture being controlled by the optimization parameter r_D

- if $r_D = 1$, $P(A|D) = P(A)$ and $P(A|B, D) = P(A|B)$, an independent new realization is generated
- if $r_D = 0$, the current realization is retained as shown previously.

Algorithm summary

The proposed algorithm to integrate production data (D) and mp geological information (B) proceeds as follows

- Define a training image depicting the desired geological continuity (information B)
- Using the snesim algorithm: generate an initial model $i^{(o)}(\mathbf{u}), \mathbf{u} \in Res., l = 0$.
- Iterate, $l = 1, \ldots, Lmax$,
  - Define a transition matrix Eqs. (2).
  - Perform a one-parameter optimization on r_D that provides the best match to the data D, then draw model, the probability $P(A|D)$ is then given by Eq. 6. This step requires multiple runs of the cosnesim algorithm and the flow simulator.
  - Derive the conditional probability from Eq. (1).
  - Make a final run of the cosnesim algorithm to generate a model $i_{r_D}^{(l+1)}(\mathbf{u})$

Application examples

Quarter 5-spot

A set of applictation examples illustrate the proposed approach. Consider the 2D horizontal reference model in Fig. 4 consisting of diagonal elliptical bodies of high permeability (750 mD) in a low permeability matrix (150 mD). We assume that the values of 150/750 mD are known, while the placement of the high permeability bodies is not known. A training

image reflecting knowledge about the elliptical shapes is generated using a Boolean program ellipsim [15], see Fig. 1 .

The production data D is generated by placing an injector well in the lower left corner which injects water in an initially oil saturated reservoir and a producer located in the upper right corner. We use a simple black oil model, unbalanced production with the injector at constant rate of 700 STB/day. No flow boundary conditions are assumed. Fluid properties and density are assumed invariant with pressure. Capillary effects are ignored. Connate water saturation is 0.15. Typical relative permeability curves are used. Initial reservoir pressure is set at 655 psi. Grid cells size is 10 ft. A finite difference simulator "Eclipse"[16] is used. The target production data D is the fractional flow of water observed in the producing well as function of time. It appears that water breaks through after about 15 days as shown in Fig. (6). The task is to generate solutions that honor the production data and the elliptical structures depicted by the training image of Fig. 1.

Fig. 5 shows the decrease in the objective function during the outer iteration (l) also shown is the optimal value $r_D^{opt,(l)}$ for each iteration (l). The objective function measures the squared difference of fractional flow data and model and has been standardized to one in Fig. 5 for the initial model. After 9 iterations a satisfactory match to the production data is found as shown in Fig. 6. While the initial model fails to capture the connectivity of flow facies between injector and producer well, the final history match appears visually to have similar connectivity between injector and producer as the reference model. Fig. 8 provides more insight into the the optimization of the r_D parameter. Each outer iteration (l) consists of an inner iteration to obtain the best r_D. On average 8 function evaluations (flow simulations) are required to perform such optimization. It appears that several local minima may occur.

Ten history matched models are generated using the above described methodology of which 4 selected models are shown in Fig. 9. The average of these 10 realizations is shown in Fig. 10. The fuzzy nature of Fig. 10 demonstrates that the fractional flow data is not a strong constraint on the resulting reservoir models.

To investigate the flexibility of the approach in terms of prior models, we apply our approach to other types of geological heterogeneities. First consider the reference model in Fig. 11 depicting a population of fractures. Production data D similar to those obtained for

the elliptical bodies case is generated by forward simulation on the reference set, providing the fractional flow of water versus time measurements shown in Fig. 12. Convergence to an acceptable history match is obtained after only 3 iterations. The initial guess plus the 3 iterations are shown in Fig. 13 and the history match shown in Fig. 12. The training image used to obtain these results is shown in Fig. 14.

A final example concerns a reference model containing channels as shown in Fig. 15. The results are show in Figs. 16 to 18.

5-spot case

Finally, we present a larger case of a 100×100 reference model shown in Fig. 19. Boundary conditions, grid and fluid specifications are the same as before, only now a full 5-spot configuration is used. The permeability constrast is now higher with 1500mD for facies 1 and 50 mD for facies 0. The Injector is located in the middle, producing well 1 in bottom left, well 2 in bottom right, well 3 in top left, well 4 in top right.

Fig. 19 shows a good connection between the injector and producing wells 1 and 4, a poor connection to producing wells 2 and 3, exhibiting later breakthrough. To match the fractional flow of all 4 wells jointly, our objective function measures the squared difference between fractional flow at all 4 wells. Fig. 21 shows that the objective function is significantly lowered after 8 iterations. The initial model, history matched model and some selected iterations are shown in Fig. 20. While the initial model appears to lack the strong connectivity between injector and producing well 1, the final history matched results shows a connectivity similar to the reference model. Fig. 22 show that the history matched is largely satisfactory for all wells.

Discussion and conclusions

In this paper we present a new geostatistical approach to history matching. The purpose of using geostatistics is to integrate geological information jointly with production data. Production data brings only a limited constraint to the reservoir permeability, particularly in

strongly heterogeneous media, hence prior geological information must be used to quantify the geological patterns deemed relevant. If geology is ignored, the resulting history matched models are often too smooth and might have limited prediction power.

Multiple-point geostatistics is used to introduce any type of geology that can be quantified in a training image into the history matching process. A simple Markov chain moves realizations that are consistent with the geology depicted in the training image to final history match. The approach is generic on two fronts: one can use the same algorithm (code) for different geological heterogeneities (cross-bedding, channels, fractures) and for different flow processes (black oil, compositional, streamlines). The essential input required are a training image and a flow simulator. No tuning parameters are needed. The code used to run all of the above examples was kept unchanged.

Certain limitations exist in the current method but can be dealt with as follows

- The theory presented deals only with two facies. If more facies are present we can extend the method in two ways.

  1. Consider K facies $s_k, k = 1, \ldots, K$, then define a set of indicator variables

  $$I(\mathbf{u}, s_k) = \begin{cases} 1 & \text{if facies } s_k \text{ occurs} \\ 0 & \text{else} \end{cases}$$

  In the algorithm we can therefore work sequentially on each variable $I(\mathbf{u}, s_k)$ by perturbing a single facies s_k versus all other facies grouped together in one class.

  2. We can consider more than one parameter r_D, namely a set of parameters $r_D(k)$ for each facies, and jointly perform optimization on the set of parameters.

- The permeability for each facies is known and constant. We can solve this problem by a hierarchical history matching process, where the iteration consists of two steps: in the first steps one perturbs facies with constant permeability, in the second step one perturbs the permeability while the facies remain frozen. For the second step one could for example apply history matching by gradual deformation[3].

Nomenclature

$\mathbf{u}$: (x, y, z)

A: an event: for example channel occurs at $\mathbf{u}$

B: another event: for example channel occurs at $\mathbf{u}_1$ **and** shale occurs at $\mathbf{u}_2$

$P(A|B)$: probabibility that event A occurs *given* one knows that B occurs

D: production data

C: seismic data

(l): iteration counter for outer loop

References

[1] WEN, X-H., DEUTSCH, C. and CULLICK, A.S., Integrating pressure and fractional flow data in reservoir modeling with fast streamline based inverse methods, paper SPE 48971 prepared for presentation at the 1998 SPE Annual Technical Conference and Exhibition, New Orleans, 27-30 September.

[2] VASCO, D.W., YOON, S. and DATTA-GUPTA, A., Integrating dynamic data into high resolution reservoir models using streamline-based analytic sensitivity coefficients, paper SPE 49002 prepared for presentation at the 1998 SPE Annual Technical Conference and Exhibition, New Orleans, 27-30 September.

[3] HU, L.Y and BLANC, G., Constraining a reservoir facies model to dynamic data using a gradual deformation model. paper B-01 prepared for presentation at the 6th European Conference on Mathematics of Oil Recovery (ECMOR VI), September 8–11, Peebles, Scotland, 1998.

[4] WU, Z, REYNOLDS, A.C. and OLIVER, D.S, Conditioning geostatistical models to two-phase production data. paper SPE 49003 prepared for presentation at the 1998 SPE Annual Technical Conference and Exhibition, New Orleans, 27-30 September.

[5] TRAN, T., DEUTSCH, C.V. and XIE, Y., Direct Geostatistical Simulation With Multiscale Well, Seismic, and Production Data, paper SPE 71323 prepared for presentation at the 2001 SPE Annual Technical Conference and Exhibition, New Orleans, September 30 – 3, October.

[6] HEGSTAD, B.K., and OMRE, H., An Inverse Problem in Petroleum Recovery: History Matching and Stochastic Reservoir Characterisation, proceedings ECMI96 conference, Copenhagen, June 25-29, 1996.

[7] CAERS, J., KRISHNAN, S., WANG, Y and KOVSCEK, A.R., A geostatistical approach to streamline-based history matching. Paper submitted to SPEJ, 2001.

[8] CAERS, J. and JOURNEL, A.G., Stochastic reservoir modeling using neural networks trained on outcrop data. paper SPE 49026 prepared for presentation at the 1998 SPE Annual Technical Conference and Exhibition, New Orleans, 27-30 September.

[9] STREBELLE, S. Sequential simulation drawing structure from training images. Ph.D dissertation, Stanford University, Stanford, California, 2000.

[10] CAERS, J. AND ZHANG, T. Multiple-point geostatistics: a quantitative vehicle for integrating geologic analogs into multiple reservoir models. To be published in ”Integration of outcrop and modern analogs in reservoir modeling, AAPG memoir, 2002.

[11] ISAAKS, E. The application of Monter Carlo methods to teh analysis of spatially correlated data. PhD dissertation, STanford University, Stanford, California, 1990.

[12] GOMEZ-HERNANDEZ, J., and SRIVASTAVA, S. ISIM3D: an ANSI-C three dimensional multiple indicator conditional simulation program. Computers and Geosscience 16, 395–410, May 1990.

[13] CAERS, J., AVSETH, P. and MUKERJI, T. Geostatistical integration of rock physics, seismic amplitudes and geological models in North-Sea turbidite systems The Leading Edge, 20, 308-312 , March 2001.

[14] JOURNEL, A.G. Combining knowledge from diverse information sources: an alternative to Bayesian analysis. Submitted to Mathematical Geology, 2002.

[15] DEUTSCH, C.V. and JOURNEL, A.G., GSLIB: Geostatistical Software Library and User’s Guide. Oxford University press, 1998.

[16] ECLIPSE 100 Reference Manual, Schlumberger-Geoquest, Houston, Texas, 1998.

[17] Press, W.H., Teukolsky, S.A, Vetterling, W.T and Flannery, B.P. Numerical recipes in C. Cambridge University Press, 1992.

Figure captions

Figure 1: Example of a training image containing elliptical patterns

Figure 2: Example of a single geostatistical realization constrained to the 8 well data on the right. Patterns are borrowed from the training image of Figure 1.

Figure 3:A single parameter r_D defines the transition from an initial realization (top left) to another independent realization ($r_D = 1$, bottom right).

Figure 4: Reference ellipse model.

Figure 5: (top) decrease in the objective function during iterative inversion, (bottom) values of r_D^{opt} for each step during the iteration.

Figure 6: History match to the fraction flow data fw.

Figure 7: Some selected steps during the iterative inversion.

Figure 8: Optimization results on r_D for each of the nine iteration during the inversion.

Figure 9: A selection of four history matched realizations.

Figure 10: Average of 10 history matched models.

Figure 11: Reference fracture model.

Figure 12: Data and history match results.

Figure 13: Initial models and iterations to reach a history match.

Figure 14: Training image for the fracture model.

Figure 15: Reference channel model.

Figure 16: Initial model and selected iterations.

Figure 17: Data and history matched results.

Figure 18: Training image for the channel model.

Figure 19: Reference model for a five spot case: injector located in the middle, well 1 in bottom left, well 2 in bottom right, well 3 in top left, well 4 in top right.

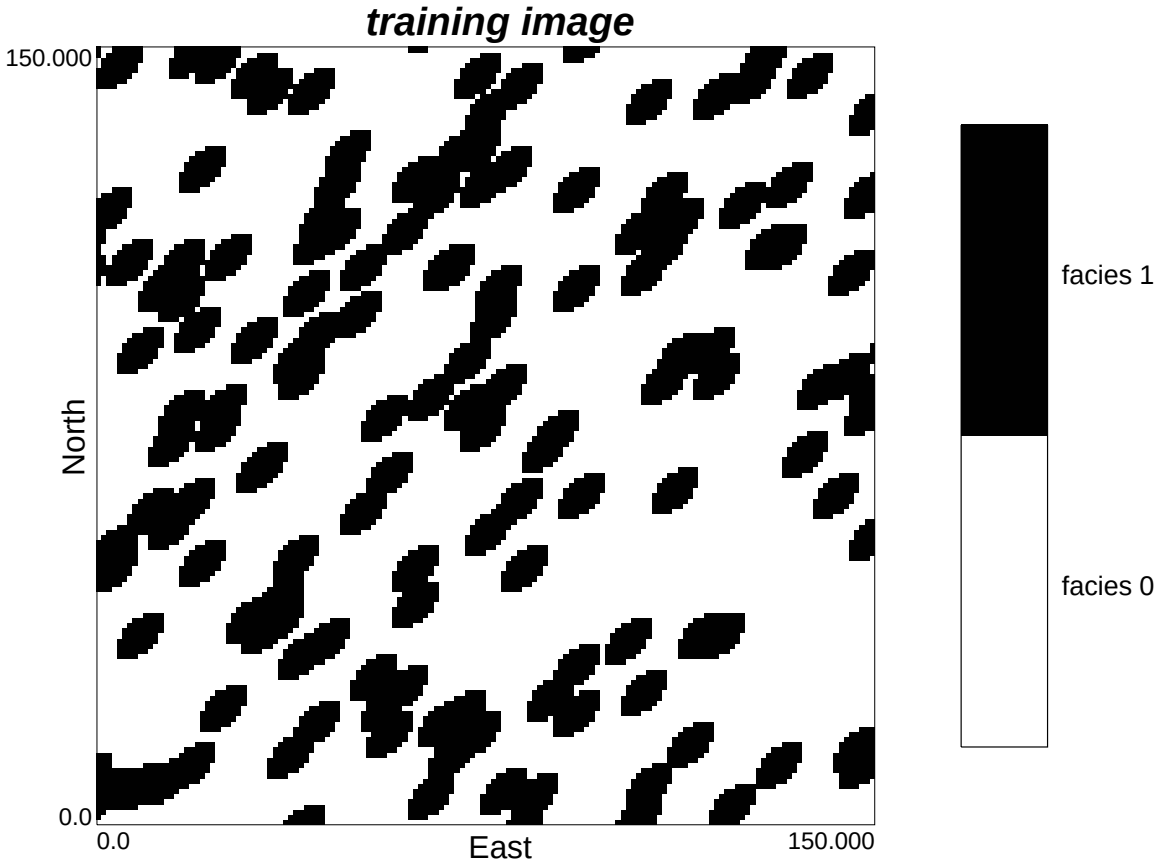

Figure 1: Example of a training image containing elliptical patterns

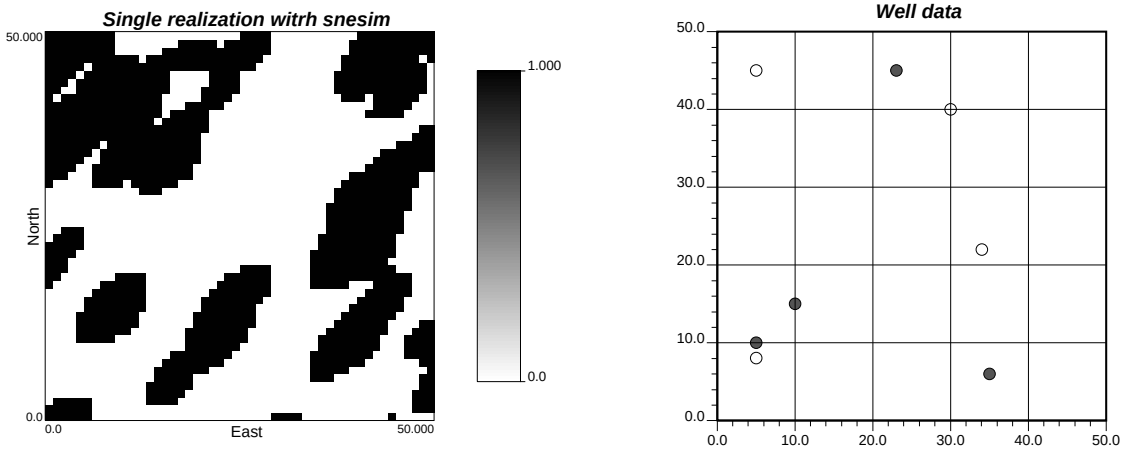

Figure 2: Example of a single geostatistical realization constrained to the 8 well data on the right. Patterns are borrowed from the training image of Figure 1

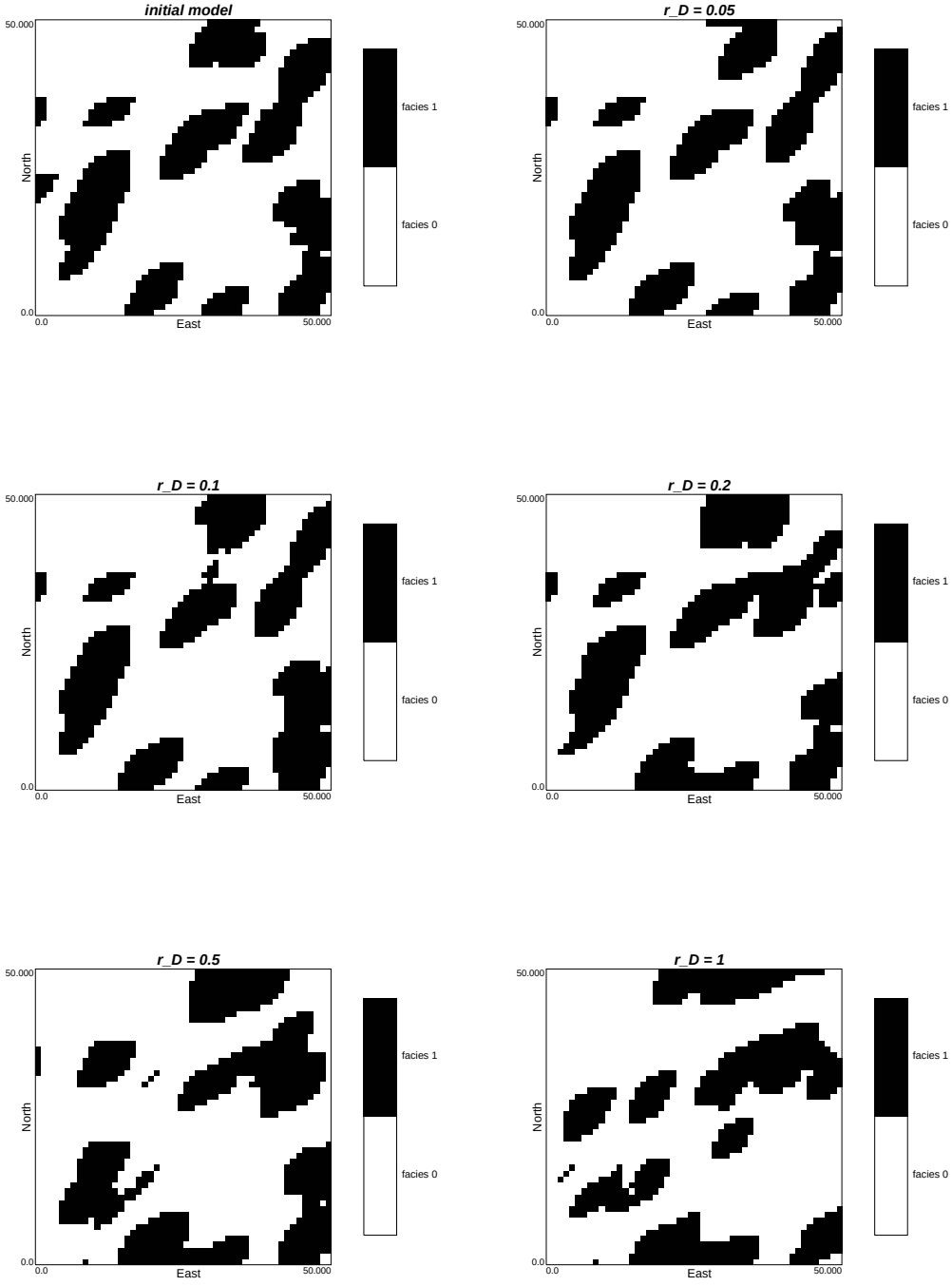

Figure 3: A single parameter r_D defines the transition from an initial realization (top left) to another independent realization ($r_D = 1$, bottom right)

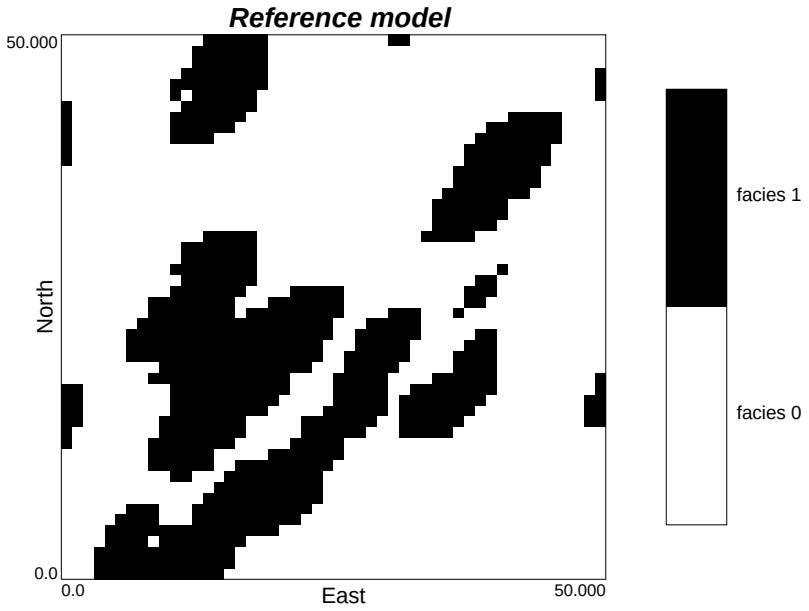

Figure 4: Reference model

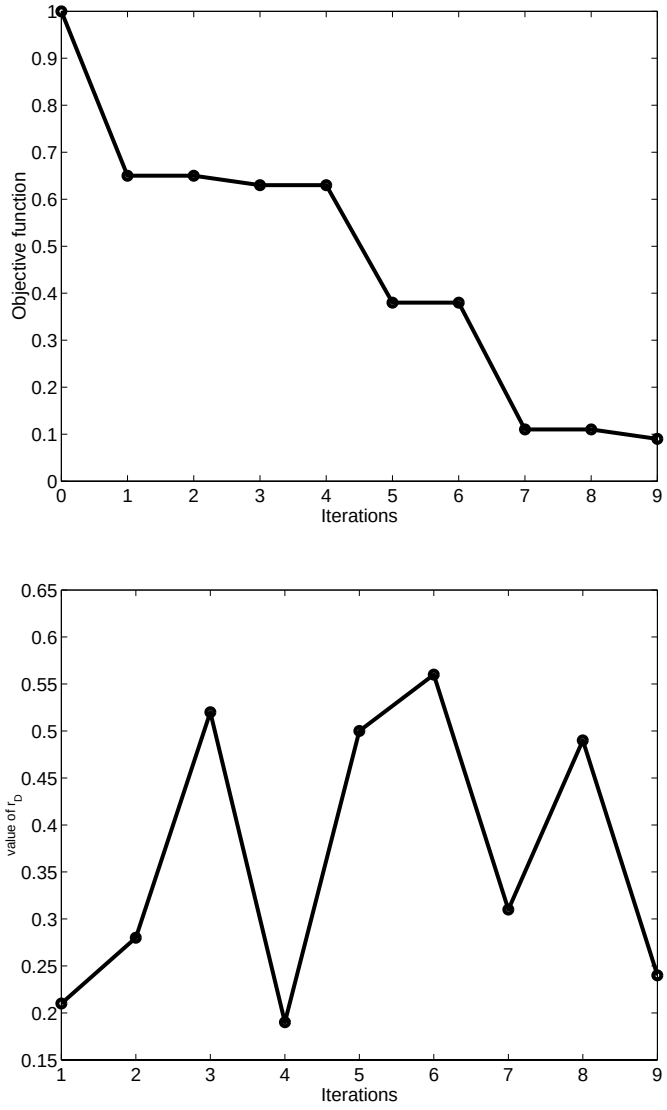

Figure 5: (top) decrease in the objective function during iterative inversion, (bottom) values of r_D^{opt} for each step during the iteration.

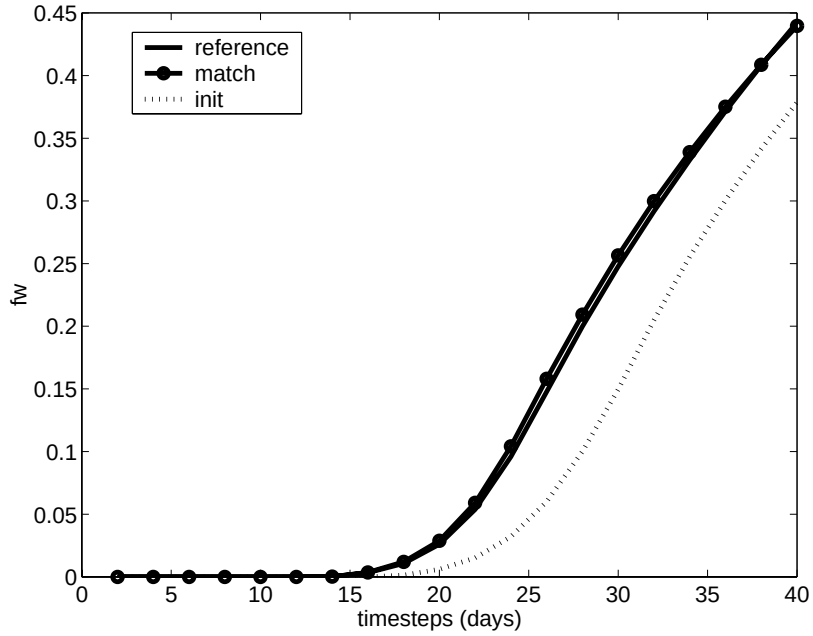

Figure 6: History match to the fraction flow data fw.

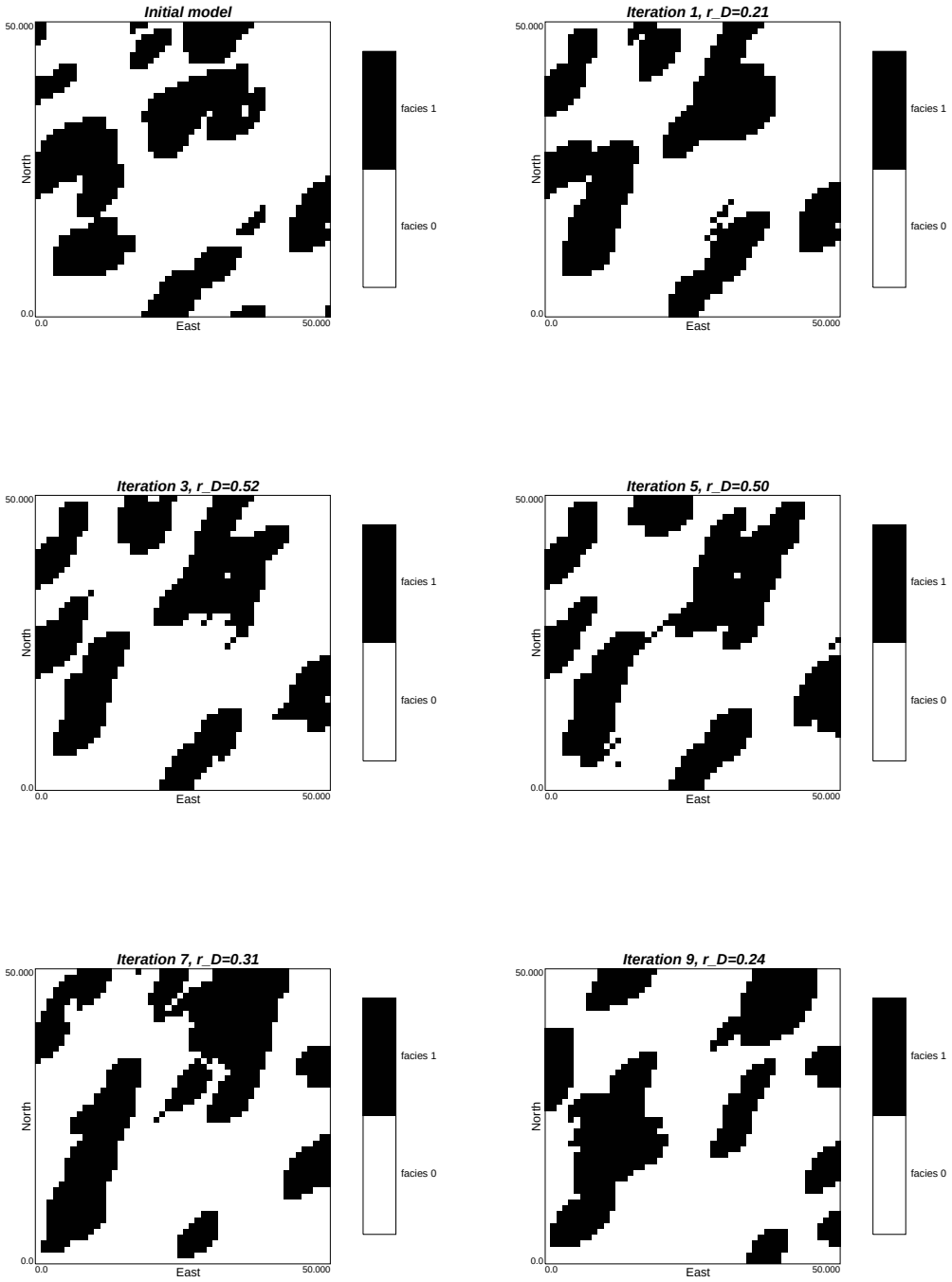

Figure 7: Some selected steps during the iterative inversion.

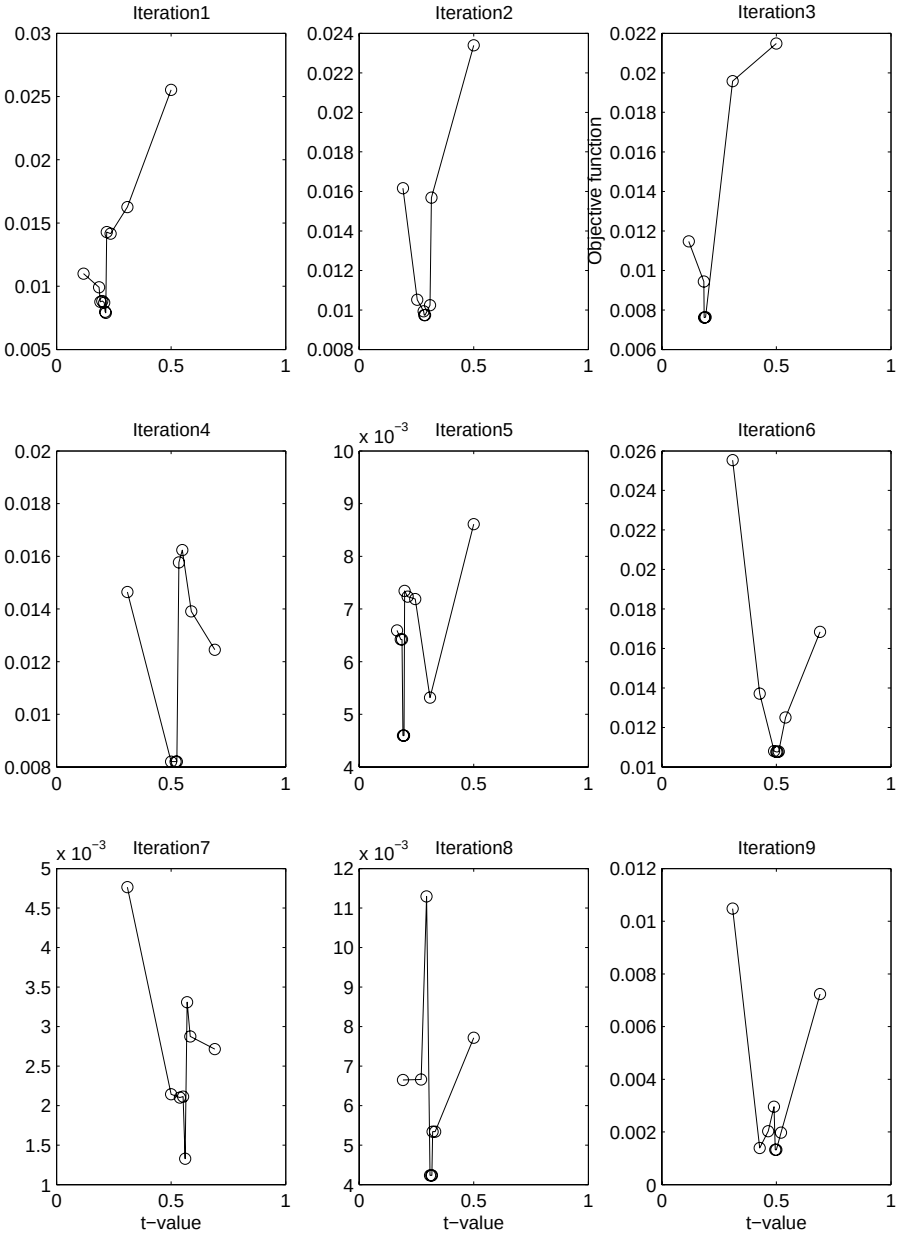

Figure 8: Optimization results on r_D for each of the nine iteration during the inversion.

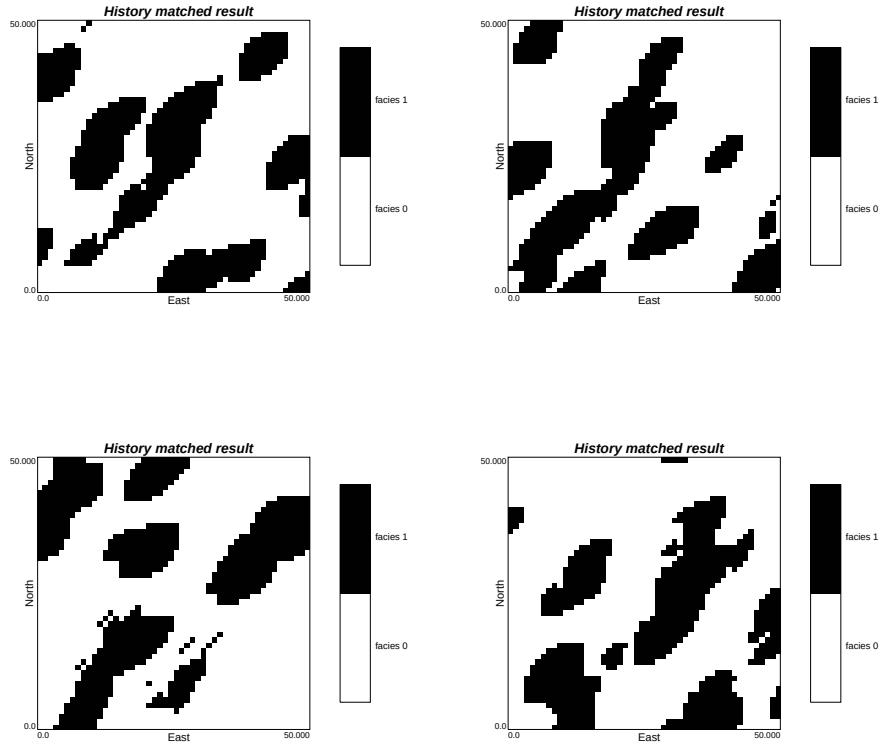

Figure 9: A selection of four history matched realizations.

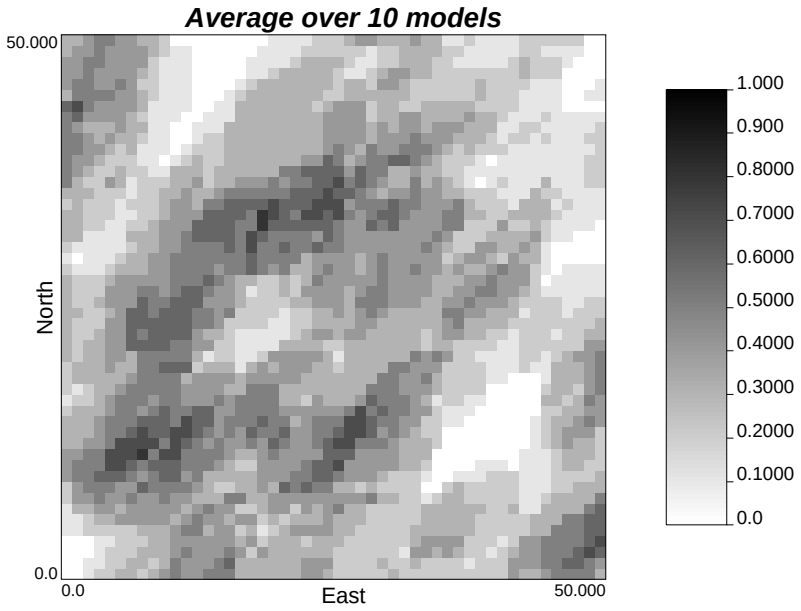

Figure 10: Average of 10 history matched models

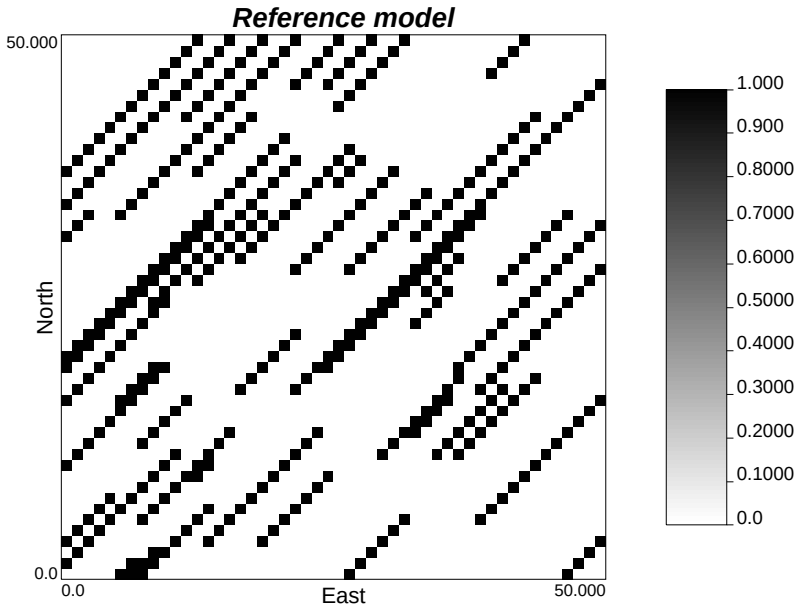

Figure 11: Reference fracture model.

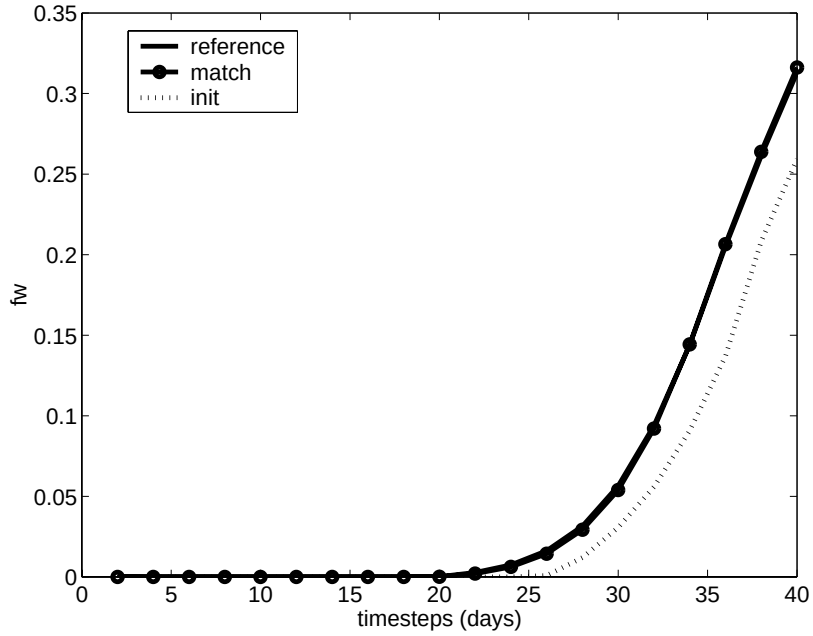

Figure 12: Data and history match results.

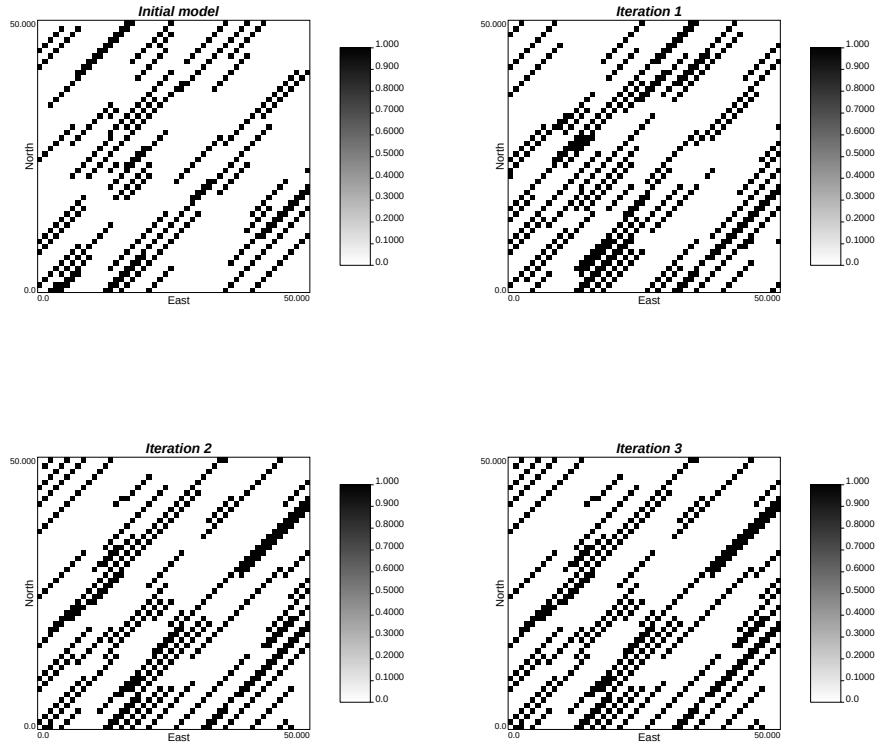

Figure 13: Initial models and iterations to reach a history match.

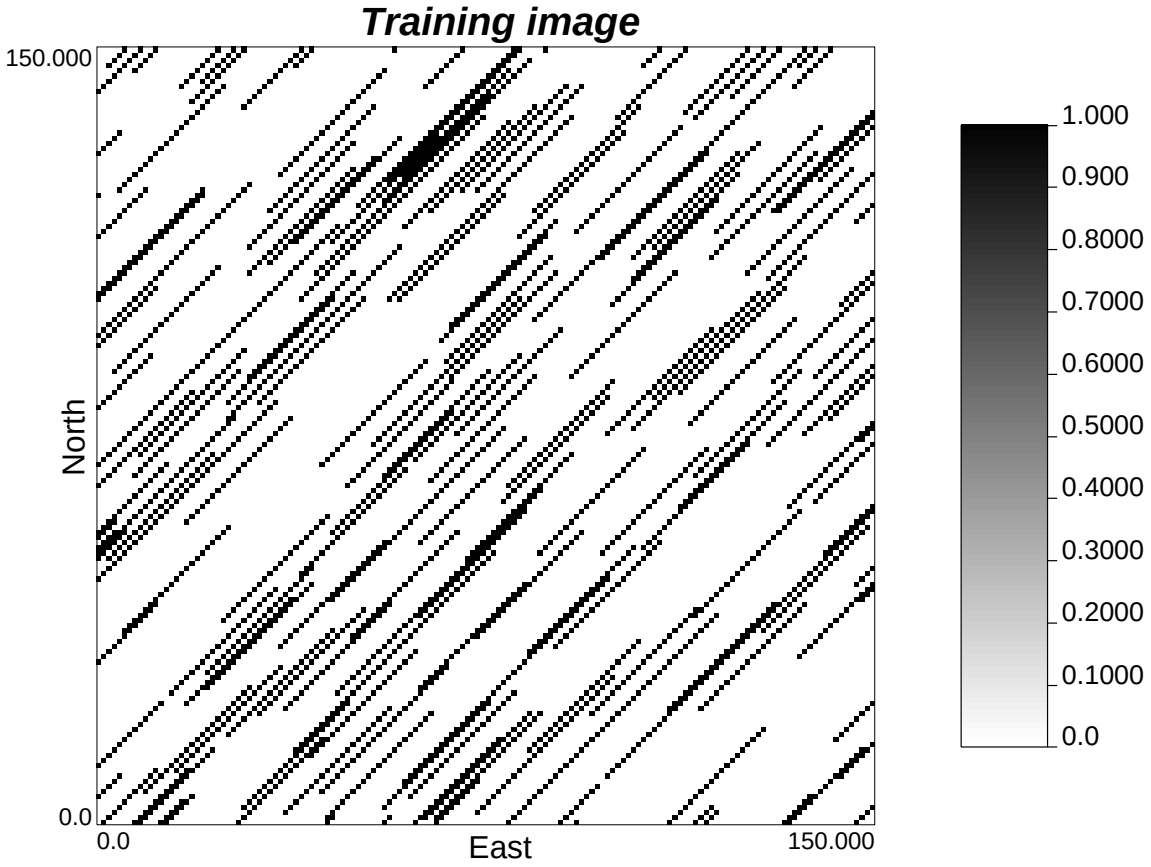

Figure 14: Training image for the fracture model

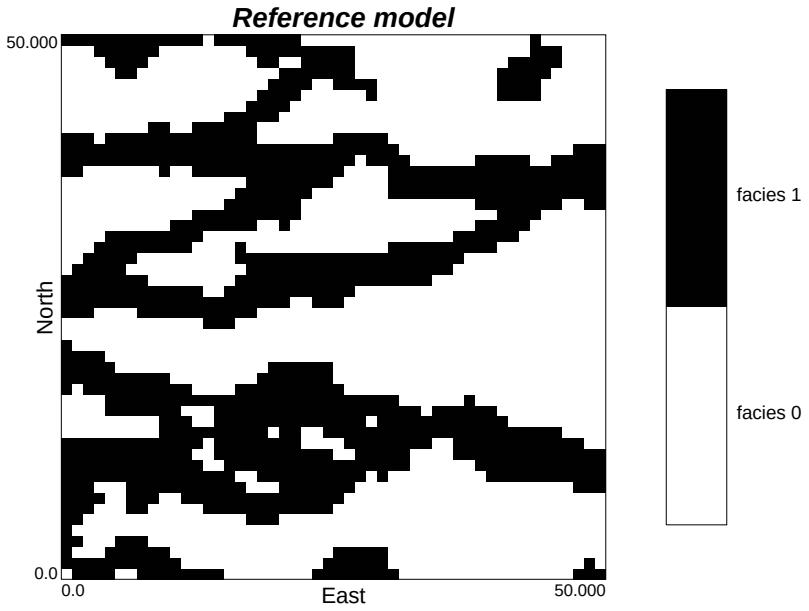

Figure 15: Reference channel model.

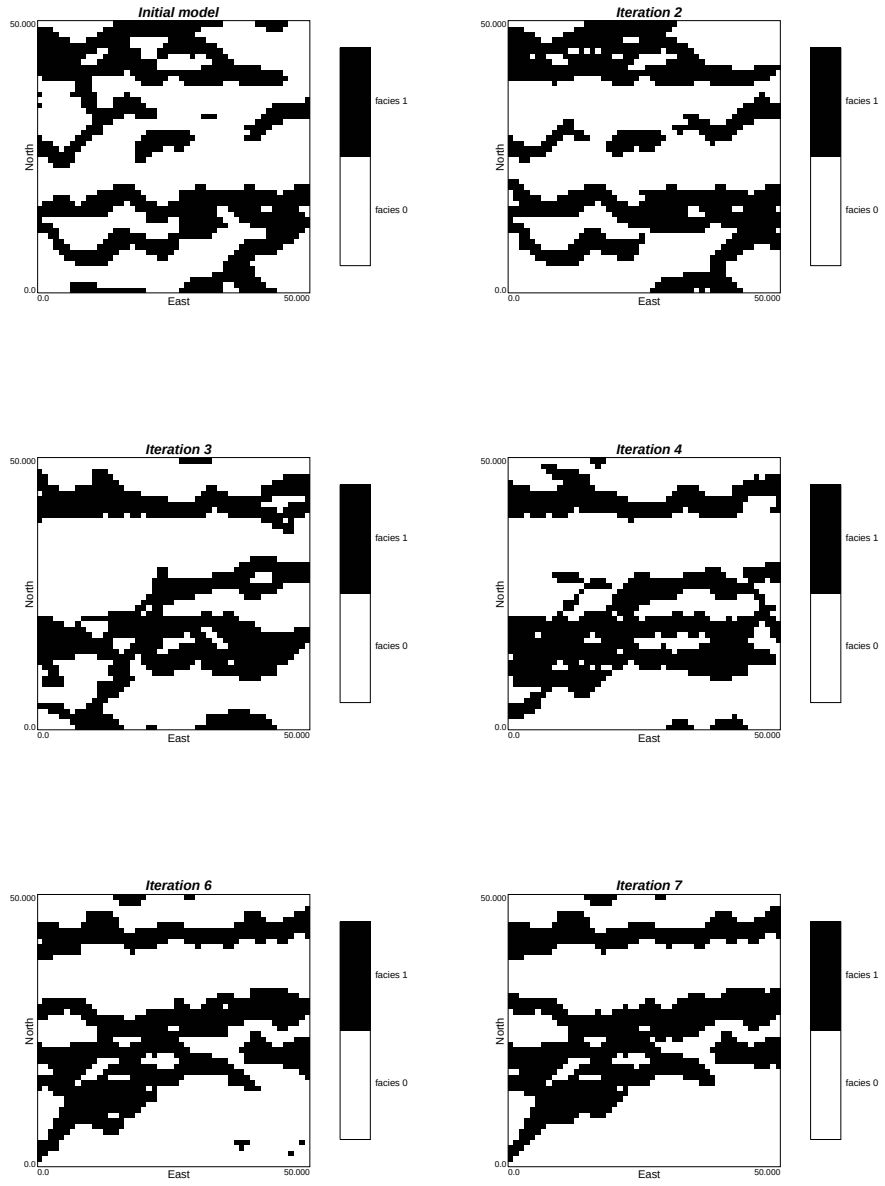

Figure 16: Initial model and selected iterations

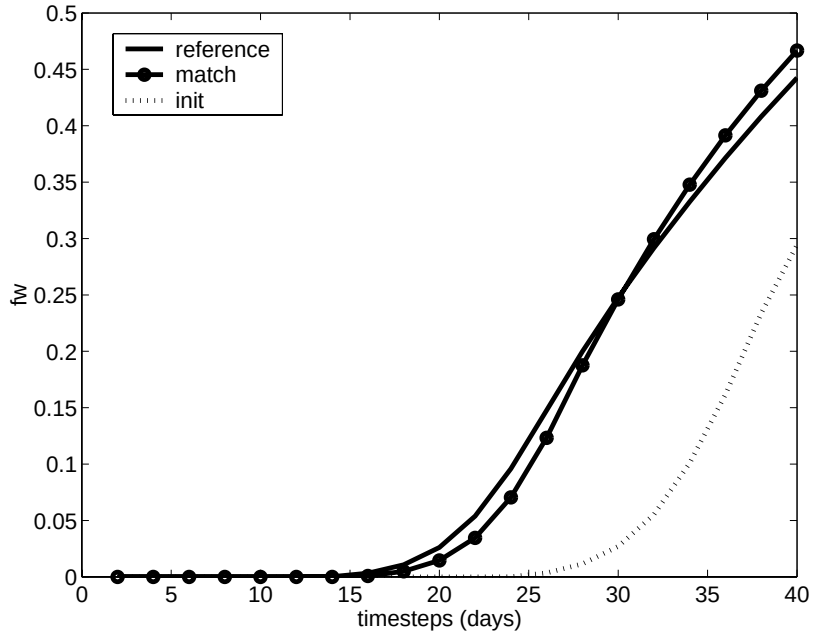

Figure 17: Data and history matched results.

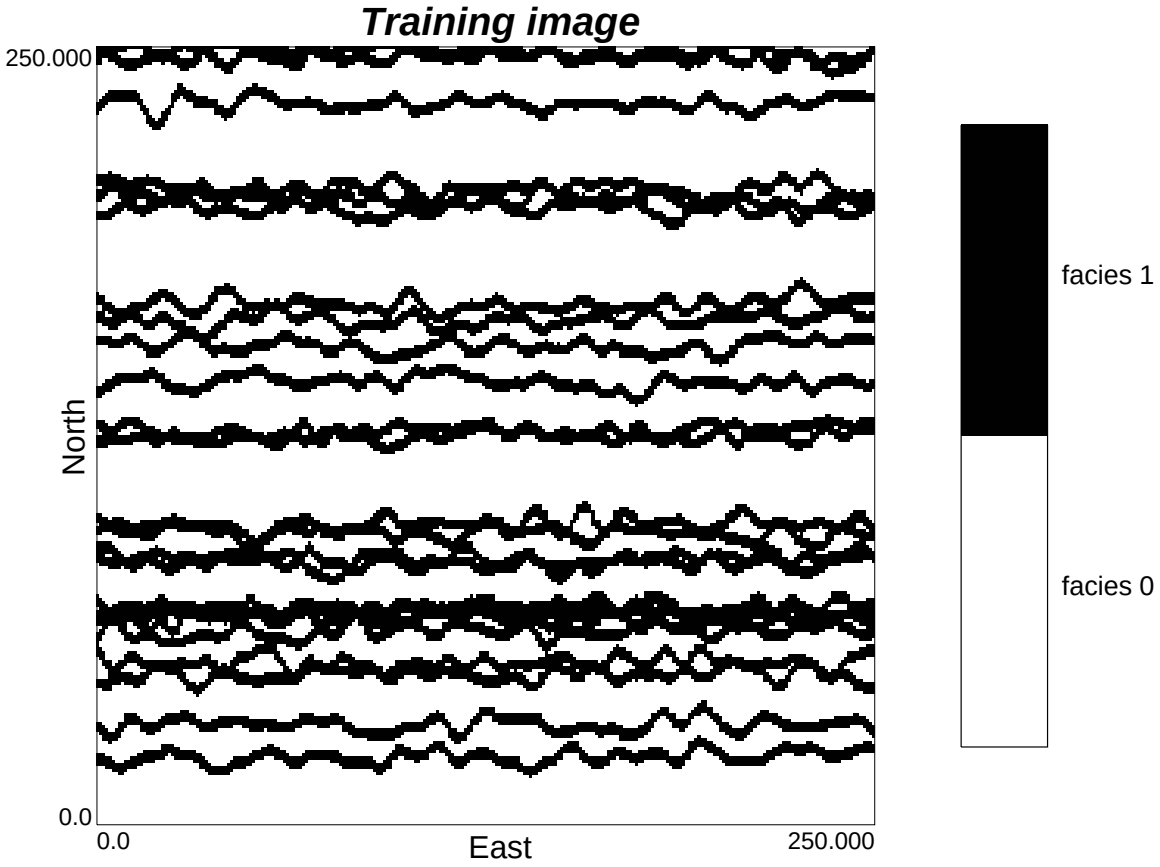

Figure 18: Training image for the channel model

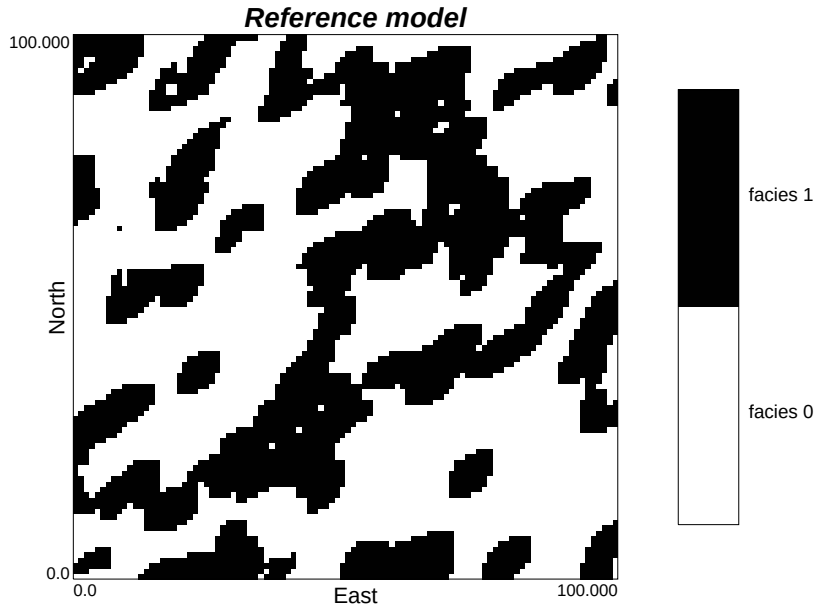

Figure 19: Reference model for a five spot case: injector located in the middle, well 1 in bottom left, well 2 in bottom right, well 3 in top left, well 4 in top right

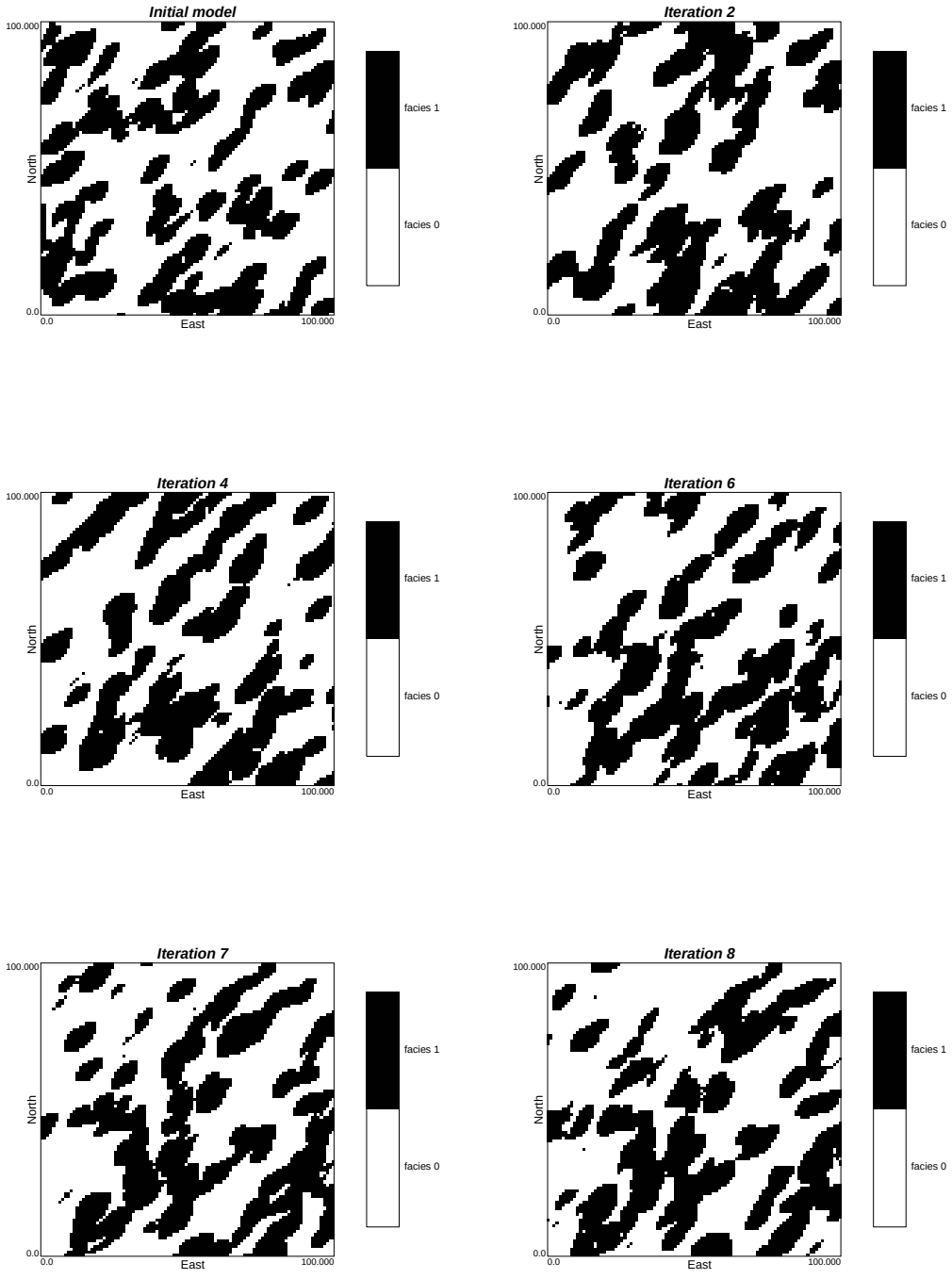

Figure 20: Initial model, history match and some selected iterations

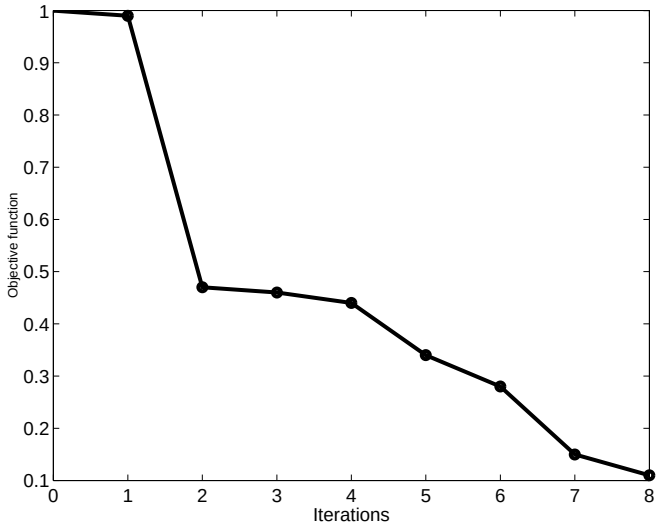

Figure 21: Decrease of the objective function

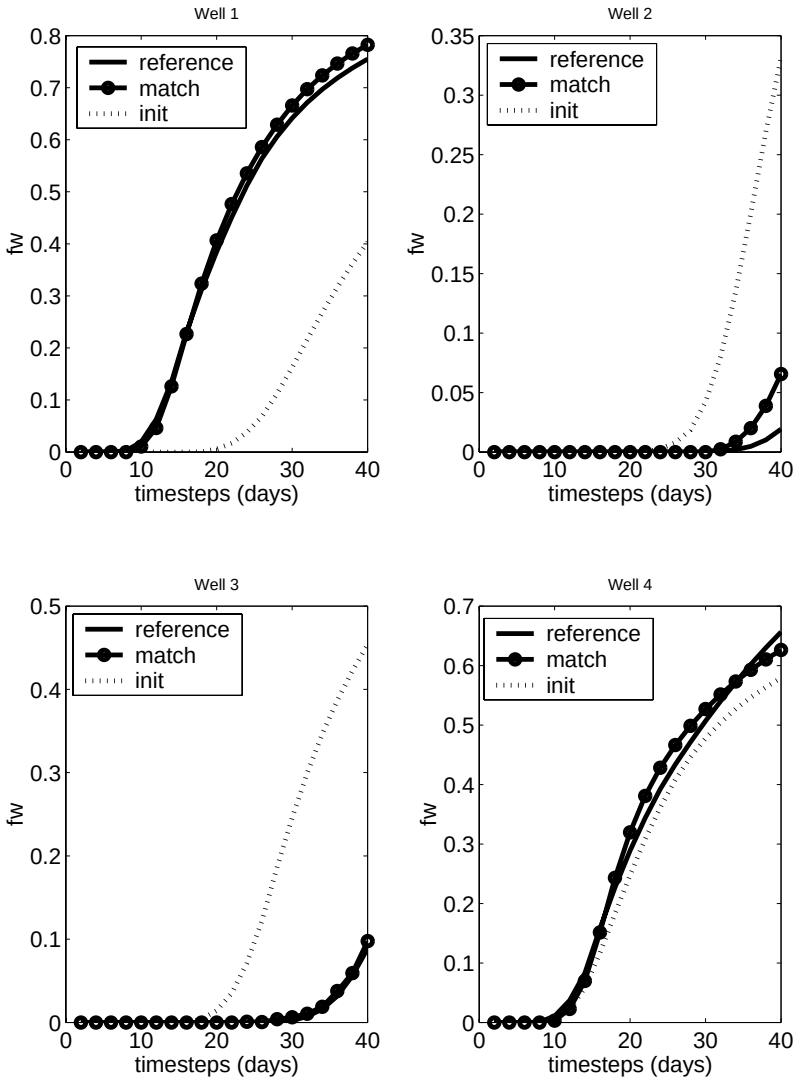

Figure 22: History matched results for all 4 wells